

# Nonlinear surface waves in left-handed materials

Ilya V. Shadrivov, Andrey A. Sukhorukov, and Yuri S. Kivshar  
*Nonlinear Physics Group, Research School of Physical Sciences and Engineering,  
Australian National University, Canberra ACT 0200, Australia\**

Alexander A. Zharov  
*Institute for Physics of Microstructures, Russian Academy of Sciences, Nizhny Novgorod 603950, Russia*

Allan D. Boardman and Peter Egan  
*Department of Physics, University of Salford, Salford M5 4WT, United Kingdom*

We study both linear and nonlinear surface waves localized at the interface separating a *left-handed medium* (i.e. the medium with both negative dielectric permittivity and magnetic permeability) and a conventional (or *right-handed*) dielectric medium. We demonstrate that the interface can support both TE- and TM-polarized surface waves—*surface polaritons*, and we study their properties. We describe the intensity-dependent properties of *nonlinear surface waves* in three different cases, i.e. when both LH and RH media are nonlinear and when either of the media is nonlinear. In the case when both media are nonlinear, we find two types of nonlinear surface waves, one with the maximum amplitude at the interface, and the other one with two humps. In the case when one medium is nonlinear, only one type of surface wave exists, which has the maximum electric field at the interface, unlike waves in right-handed materials where the surface-wave maximum is usually shifted into a self-focussing nonlinear medium. We study the energy flow near the surface and demonstrate the specific vortex-like structure of temporal pulses propagating along the interface, as well as discuss the possibility of tuning the wave group velocity in both the linear and nonlinear cases. We show that the group-velocity dispersion, which leads to the pulse broadening, can be balanced by nonlinearity of the media resulting in the soliton propagation.

PACS numbers: 78.68.+m, 42.65.Tg

## I. INTRODUCTION

Novel physical effects in dielectric media with both negative permittivity and negative permeability were first analyzed theoretically by Veselago [1] who predicted a number of unusual phenomena including, for example, negative refraction of waves. Such media are usually known as *left-handed (LH) media* since the electric and magnetic fields form a left set of vectors with a wave vector. The physical realization of such LH media was demonstrated only recently [2] for a novel class of engineered composite materials, now called *LH metamaterials*. Such LH materials attracted attention not only due to their recent experimental realization and a number of unusual properties observed in experiment, but also due to the expanding debates on the use of a slab of a LH metamaterial as a perfect lens for focusing both propagating and evanescent waves [3].

The concept of a perfect lens was first introduced by Pendry [4], who suggested the idea that a slab of a lossless negative-refraction material can be used for creating a perfect image of a point source. Although the concept of a perfect lens is a result of an ideal theoretical model employed in the analysis [4], the resolution limit of a LH slab was shown to be independent on the wavelength of the electromagnetic wave (but can be determined by other sources such as loss, spatial dispersion, etc.), so that the resolution can be indeed much better than the resolution of a conventional lens [5].

The improved resolution of a LH slab and the corresponding amplification of evanescent modes in a lossy LH material, can be understood from simple physics. Indeed, the near field of an image, which can not be focused by a normal lens, can be transferred through the slab of a LH material due to the excitation of *surface waves* (or surface polaritons) at both interfaces of the slab. Therefore, as the first major step in the understanding of the amplified transmission of the evanescent waves, as well as other unusual properties of the LH materials, it is important to study the properties of different types of surface waves that can be excited at the interfaces between LH and conventional (or right-handed, RH) media. Some preliminary studies in this direction included calculation of the *linear* dispersion properties of modes localized at a single interface or in a slab of LH material [6–9].

In this paper, we present a comprehensive study of the properties of both *linear and nonlinear surface waves* at the interface between semi-infinite materials of two types, left- and right-handed ones, and demonstrate a number of unique features of surface waves in LH materials. In particular, we show the existence of surface waves of both TE and TM polarizations, a specific feature of the RH/LH interfaces. We suggest an efficient way for engineering of the group velocity of surface waves using the nonlinearity of the media. Additionally, we reveal a distinctive vortex-like structure of the energy flow in a localized surface wave propagating along the interface. The dispersion broadening of the pulse can be compensated by

the nonlinearity, thus leading to the formation of surface-polariton solitons at the RH/LH interfaces.

The paper is organized as follows. In Sec. II we study the properties of surface waves in the linear regime. We consider the most general case of an interface between linear RH and LH media, and present a classification of TE- and TM-polarized surface waves localized at the interface. Section III is devoted to the study of the structure and general properties of nonlinear surface waves. We describe the intensity-dependent properties of surface waves in three possible cases. In the first case, we assume that both LH and RH media are nonlinear. In the second case, the LH medium is nonlinear, but the RH medium is assumed to be linear. In the third case, the RH medium is considered to be nonlinear while the LH medium remains linear. In all these cases, we describe the nonlinear medium as that with the intensity-dependent Kerr-like dielectric permittivity. In Section IV, we study the frequency dispersion of nonlinear surface waves. In particular, we demonstrate that the group velocity of surface waves can effectively be engineered by using the intensity-dependent dispersion. A detailed analysis is carried out for the example of nonlinear RH and linear LH media. Finally, in section V we discuss the structure of the energy flow carried by a localized wave packet of a surface-wave mode along the interface, and we demonstrate analytically that it has a distinct vortex-like structure. We also describe the properties of nonlinear localized modes propagating along the interface, and predict the existence of surface polariton solitons.

## II. LINEAR SURFACE WAVES

### A. Model

*Linear surface waves* are known to exist, under certain special conditions, at the interface separating two different dielectric media. In particular, the existence of TM-polarized surface waves requires that the dielectric constants of two dielectric materials separated by an interface have different signs, whilst for TE-polarized waves the magnetic permeability of the materials should be of different signs (see, e.g. Ref. [10] and references therein). Materials with negative  $\epsilon$  are readily available (e.g., metals excited below a critical frequency), whilst the materials with negative  $\mu$  were not known until recently. This explains why only TM-polarized surface waves have been of interest over the last few decades.

Some preliminary studies of the properties of surface waves excited at the interface separating a LH metamaterial and a dielectric have been recently reported by several groups [6, 8, 9, 11]. Moreover, the novel concept of a perfect lens [4] is based on the properties of surface waves at the interfaces of a LH slab. This calls for a systematic analysis of the existence and properties of surface waves in LH materials, including the study of the nonlinear regime and nonlinear surface waves.

In this paper, we consider an interface between the RH (medium 1) and LH (medium 2) semi-infinite media, as shown in the inset of Fig. 1. The propagation of monochromatic waves with the frequency  $\omega$  is governed by the scalar wave equation, which for the case of the TE waves is written for the  $y$ -component of the electric field,

$$\left[ \frac{\partial^2}{\partial z^2} + \frac{\partial^2}{\partial x^2} + \frac{\omega^2}{c^2} \epsilon(x) \mu(x) - \frac{1}{\mu(x)} \frac{\partial \mu(x)}{\partial x} \frac{\partial}{\partial x} \right] E_y = 0. \quad (1)$$

In the case of the TM waves, the scalar wave equations is written for the  $y$ -component of magnetic field,

$$\left[ \frac{\partial^2}{\partial z^2} + \frac{\partial^2}{\partial x^2} + \frac{\omega^2}{c^2} \epsilon(x) \mu(x) - \frac{1}{\epsilon(x)} \frac{\partial \epsilon(x)}{\partial x} \frac{\partial}{\partial x} \right] H_y = 0. \quad (2)$$

In Eqs. (1) and (2), the functions  $\epsilon(x)$  and  $\mu(x)$  are dielectric permittivity and magnetic permeability in a bulk medium, respectively;  $\omega$  is the angular wave frequency, and  $c$  is the speed of light in vacuum. The nonzero components of magnetic field and of electric field are found from the Maxwell's equations, in the case of the TE waves

$$H_z = -\frac{ic}{\omega \mu} \frac{\partial E_y}{\partial x}; \quad H_x = \frac{ic}{\omega \mu} \frac{\partial E_y}{\partial z}, \quad (3)$$

and the TM waves

$$E_z = \frac{ic}{\omega \epsilon} \frac{\partial H_y}{\partial x}; \quad E_x = -\frac{ic}{\omega \epsilon} \frac{\partial H_y}{\partial z}, \quad (4)$$

respectively. For the piecewise linear medium, the equations (1) and (2) can be rewritten for each of the media in the following form:

$$\left[ \frac{\partial^2}{\partial z^2} + \frac{\partial^2}{\partial x^2} + \frac{\omega^2}{c^2} \epsilon_{1,2} \mu_{1,2} \right] E_y = 0, \quad (5)$$

for the TE waves, and

$$\left[ \frac{\partial^2}{\partial z^2} + \frac{\partial^2}{\partial x^2} + \frac{\omega^2}{c^2} \epsilon_{1,2} \mu_{1,2} \right] H_y = 0, \quad (6)$$

for the TM waves. Solutions of Eqs. (5) and (6) in each medium for localized modes, i.e. those propagating along the interface and decaying in transverse direction, have the standard form

$$(E_y, H_y) = A_0 e^{ihz - \kappa_{1,2}|x|}, \quad (7)$$

where  $A_0$  is the wave amplitude at the interface,  $h$  is a propagation constant,

$$\kappa_{1,2} = \left[ h^2 - \epsilon_{1,2} \mu_{1,2} \left( \frac{\omega}{c} \right)^2 \right]^{1/2}$$

is the transverse wave number which characterizes the inverse decay length of the surface wave in the corresponding medium.

The boundary conditions for the tangential components of the electric and magnetic fields should be applied

at the interface between two media, giving the dispersion relations for surface waves at the interface [6],

$$\frac{\kappa_1}{\mu_1} + \frac{\kappa_2}{\mu_2} = 0, \quad (8)$$

and

$$\frac{\kappa_1}{\epsilon_1} + \frac{\kappa_2}{\epsilon_2} = 0, \quad (9)$$

for the cases of the TE- and TM-polarized surface waves, respectively.

### B. Properties of surface waves

For the analysis presented below, it is convenient to rewrite the dispersion relations (8) and (9) in the following form,

$$h^2 = \epsilon_1 \mu_1 \left( \frac{\omega}{c} \right)^2 \frac{Y(Y-X)}{(Y^2-1)}, \quad (10)$$

and

$$h^2 = \epsilon_1 \mu_1 \left( \frac{\omega}{c} \right)^2 \frac{X(X-Y)}{(X^2-1)}, \quad (11)$$

respectively, where we introduced the dimensionless normalized ratios  $X = |\epsilon_2|/\epsilon_1$  and  $Y = |\mu_2|/\mu_1$  which characterize the relative properties of the media creating the interface. In terms of these new parameters, the existence regions for surface waves can be determined from the condition of surface wave localization, i.e. when the transverse wave numbers  $\kappa_{1,2}$  are real,  $h > \max\{\omega\epsilon_1\mu_1/c, \omega\epsilon_2\mu_2/c\}$ . Existence regions for both polarizations of surface wave are presented on the parameter plane  $(X, Y)$  in Fig. 1. Along with the polarization, we denote the type of the wave, *forward* or *backward*, which we discuss below in Sec. II C. We notice that there exist no regions where both TE- and TM-polarized waves co-exist simultaneously, but both types of surface wave can be supported by the same interface for different parameters, e.g. for different frequencies.

One of the distinctive properties of the LH materials which has been demonstrated experimentally is their specific frequency dispersion. To study the dispersion of the corresponding surface waves, it is necessary to select a particular form of the frequency dependence of dielectric permittivity and magnetic permeability of the LH medium. A negative dielectric permittivity is selected in the form of the commonly used function for plasmon investigations [10] and a negative permeability is constructed in an analogous form (see, e.g. Ref. [6]), i.e.

$$\epsilon_2(\omega) = 1 - \frac{\omega_p^2}{\omega^2}, \quad \mu_2(\omega) = 1 - \frac{F\omega^2}{\omega^2 - \omega_r^2}, \quad (12)$$

where losses are neglected, and the values of the parameters  $\omega_p$ ,  $\omega_r$ , and  $F$  are taken to be close to the experimental data, i.e.  $\omega_p/2\pi = 10$  GHz,  $\omega_r/2\pi = 4$  GHz,

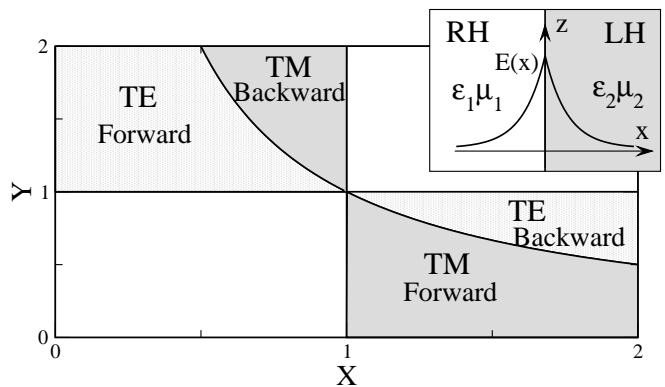


FIG. 1: Existence regions of surface waves on the parameter plane  $(X, Y)$ , where  $X = |\epsilon_2|/\epsilon_1$  and  $Y = |\mu_2|/\mu_1$ . The inset shows the problem geometry.

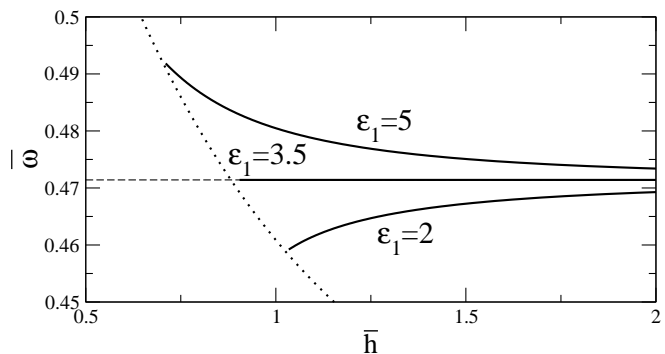


FIG. 2: Dispersion curves of the TE-polarized surface waves, for different values of  $\epsilon_1$ , shown for the normalized values  $\bar{\omega} = \omega/\omega_p$  are  $\bar{h} = hc/\omega_p$ . Dotted curves marks the dependence  $\bar{h} = \bar{\omega}\sqrt{\epsilon_2\mu_2}$ . Dashed line is the critical frequency  $\omega_1$ .

and  $F = 0.56$ . For this set of parameters, the region of the simultaneously negative permittivity and negative permeability is from 4 GHz to 6 GHz.

The dispersion curves of the TE-polarized surface wave (or surface polariton) calculated with the help of Eq. (12) are depicted in Fig. 2 on the plane of the normalized parameters  $\bar{\omega} = \omega/\omega_p$  and  $\bar{h} = hc/\omega_p$ . We notice that the structure of the dispersion curves for surface waves depends on the relation between the values of the dielectric permittivities of the two media at the characteristic frequency,  $\omega_1$ , at which the absolute values of magnetic permeabilities of two media coincide,  $\mu_1 = |\mu_2(\omega_1)|$ . The corresponding curve in Fig. 2 is monotonically decreasing for  $\epsilon_1 < |\epsilon_2(\omega_1)|$ , but it is monotonically increasing otherwise, i.e. for  $\epsilon_1 > |\epsilon_2(\omega_1)|$ . As a matter of fact, the second case was missed in the previous analysis reported in Ref. [6]. The change of the slope of the curve (the slope of the dispersion curve represents the group velocity) at the variation of the dielectric permittivity of the RH medium can be used for the group velocity engineering, which we discuss below in Sec. IV.

The critical value of dielectric permittivity  $|\epsilon_2(\omega_1)|$  for the case of a nonmagnetic RH medium ( $\mu_1 = 1$ ) is found

from the dispersion relations (8) and (12), and it has the form

$$\epsilon_c = |\epsilon_2(\omega_1)| = \left(1 - \frac{F}{2}\right) \left(\frac{\omega_p}{\omega_0}\right)^2 - 1 \quad (13)$$

For the parameters specified above, this critical value is  $\epsilon_c = 3.5$ .

The change of the dispersion curve from monotonically increasing to monotonically decreasing, shown in Fig. 2, is connected with a change in the direction of the total power flow in the wave, as discussed below.

### C. Energy flow near the interface

The energy flow is described by the Poynting vector, which defines the energy density flux averaged over the period  $T = 2\pi/\omega$ , and can be written in the form

$$\mathbf{S} = \frac{c}{8\pi} \text{Re}[\mathbf{E} \times \mathbf{H}^*], \quad (14)$$

where  $\mathbf{E}$ ,  $\mathbf{H}$  are the complex envelopes of the electric field and magnetic field of a surface wave, respectively, and the asterisk stands for the complex conjugation.

The stationary surface wave propagating along the interface has only one component of the averaged Poynting vector,  $|\mathbf{S}| = |S_z|$ . The energy flux in the RH and LH media is an integral of the Poynting vector over the corresponding semi-infinite spatial region,

$$P_1 = \int_{-\infty}^0 S_z dz = \frac{Bh}{\kappa_1} \begin{cases} 1/\mu_1; & \text{for TE,} \\ 1/\epsilon_1; & \text{for TM,} \end{cases} \quad (15)$$

$$P_2 = \int_0^{\infty} S_z dz = \frac{Bh}{\kappa_2} \begin{cases} 1/\mu_2; & \text{for TE,} \\ 1/\epsilon_2; & \text{for TM,} \end{cases} \quad (16)$$

where constant  $B$  is proportional to the mode intensity. We notice that the electromagnetic energy flow is in opposite directions at either side of the interface. The total energy flux in the  $z$ -direction is defined as the sum,  $P = P_1 + P_2$ , and it is found as

$$P = (1 - XY) \frac{Bh\omega^2 \epsilon_1 \mu_1}{\kappa_1 \kappa_2 c^2} \begin{cases} (1 + Y^2) [Y(\mu_1 \kappa_1 - \mu_2 \kappa_2)]^{-1}, \\ (1 + X^2) [X(\epsilon_1 \kappa_1 - \epsilon_2 \kappa_2)]^{-1}, \end{cases} \quad (17)$$

for the TE and TM waves, respectively. The total energy flux is positive for  $XY < 1$ , and negative for  $XY > 1$ . The surface waves are forward or backward, respectively. The corresponding types of surface waves determined from this analysis are marked in Fig. 1 as well.

## III. NONLINEAR SURFACE WAVES

### A. Nonlinear LH/RH interface

Nonlinear surface waves at the interface separating two conventional dielectric media have been analyzed extensively for several decades starting from the pioneering

paper [12]. In brief, one of the major findings of those studies is that the TE-polarized surface waves can exist at the interface separating two RH media provided that *at least one of these is nonlinear*, but that *no surface waves exist in the linear limit*.

In this section, we study nonlinear surface waves assuming that both media are nonlinear, i.e. they display a Kerr-type nonlinearity in their dielectric properties, namely

$$\epsilon_{1,2}^{NL} = \epsilon_{1,2} + \alpha_{1,2}|E|^2, \quad (18)$$

where the first term characterizes the linear properties, i.e. those in the limit of vanishing wave amplitude.

First, we should mention that the recent systematic study of nonlinear properties of metallic composites [13] suggested the possibility of hysteresis-type nonlinear effects in a structure consisting of arrays of split-ring resonators (SRRs) and wires embedded in a nonlinear dielectric medium. Such effects can also be caused by a nonlinear dielectric material placed in the slits of the SRRs, which results in the intensity-dependent capacitance of the slit. These hysteresis effects can be avoided if the structure is filled by a nonlinear dielectric material except in the SRR slits. In what follows, we consider such composite structures for which the nonlinear properties can be characterized by Eq. (18) valid far from the resonances.

For a conventional (or right-handed) dielectric medium, positive  $\alpha_1$  corresponds to a self-focusing nonlinear material, whilst negative  $\alpha_1$  characterizes defocusing effects in the beam propagation. However, this classification becomes reversed in the case of LH materials and, for example, the self-focusing LH medium corresponds to negative  $\alpha_2$ . Indeed, taking into account relation (18), we rewrite Eq. (5) for the case of the TE-polarized wave in nonlinear media as follows,

$$\frac{\partial^2 E}{\partial z^2} + \frac{\partial^2 E}{\partial x^2} + \left(\frac{\omega}{c}\right)^2 (\epsilon\mu + \mu\alpha|E|^2) E = 0. \quad (19)$$

Analyzing Eq. (19), we come to the conclusion that the type of nonlinear self-action effects is determined by the product  $\mu_2\alpha_2$ . Therefore, in the LH medium with negative  $\mu_2$  *all nonlinear effects are opposite* to those in the RH media with positive  $\mu_1$ , for the same  $\alpha$ . Below, we assume for definiteness that both LH and RH materials possess self-focusing properties, i.e.  $\alpha_1 > 0$  and  $\alpha_2 < 0$ .

We look for the stationary solutions of Eq. (19) in the form  $E_{1,2}(x, z) = \Psi_{1,2}(x) \exp(ihz)$ , where the envelopes  $\Psi_{1,2}(x)$  are found in the standard form

$$\Psi_{1,2}(x) = (\eta_{1,2}/\sqrt{\alpha_{1,2}\mu_{1,2}}) \text{sech}[\eta_{1,2}(x - x_{1,2})], \quad (20)$$

where  $\eta_{1,2} = \kappa_{1,2}c/\omega$  are normalized transverse wave numbers,  $x_{1,2}$  are centers of the *sech*-functions which should be determined from the matching conditions of continuity of the tangential components of the electric

and magnetic fields at the interface. In fact, these parameters are found from the transcendental equations

$$\tanh^2(\eta_1 x_1) = \left(1 - \frac{\alpha_1 \mu_1 \eta_2^2}{\alpha_2 \mu_2 \eta_1^2}\right) \left(1 - \frac{\alpha_1 \mu_2}{\alpha_2 \mu_1}\right)^{-1}, \quad (21)$$

and

$$\frac{\eta_2}{\mu_2} \tanh(\eta_2 x_2) = \frac{\eta_1}{\mu_1} \tanh(\eta_1 x_1). \quad (22)$$

Note, that if the parameters  $(x_1, x_2)$  correspond to one of the solutions of the equation, then  $(-x_1, -x_2)$  gives another solution. Two waves described by these solutions have the same wave number, but they correspond to different transverse structures of the surface wave, one of which has a maximum of the intensity at the interface, and the other one that has two humps shifted into the media.

In a degenerate case, when  $(\alpha_1, \mu_1, \epsilon_1) = (|\alpha_2|, |\mu_2|, |\epsilon_2|)$ , the system has an infinite number of solutions. Indeed, any  $(x, -x)$  pair will describe a stationary solution for the surface wave. Such waves have a zero total energy flux because of the symmetry of the solution.

First, we consider the surface waves in the case  $\alpha_1 = |\alpha_2|$ . The energy flow in this wave can be written in the form

$$P = P_0 \gamma \left[ \frac{\eta_1 \alpha_2 \mu_2}{\alpha_1 \mu_1^2} + \frac{\eta_2}{\mu_2} + \frac{\eta_1}{\mu_1} \left(1 - \frac{\alpha_2 \mu_2}{\alpha_1 \mu_1}\right) \tanh(\eta_1 x_1) \right], \quad (23)$$

where  $P_0 = c^2/4\pi\omega\alpha_2\mu_2$ , and  $\gamma = hc/\omega$  is the normalized wave number. The dependence of the normalized energy flux  $P/P_0$  on the parameter  $\gamma$  is shown in Fig. 3 for the cases when linear waves are forward or backward, respectively. Corresponding transverse wave structures are shown in the insets.

The linear limit corresponds to the case  $P \rightarrow 0$  when  $x_1 \rightarrow +\infty$  and  $x_2 \rightarrow -\infty$ . Moving along the curves, the centers of the *sech*-functions move toward the interface and at the point with  $dP/d\gamma = \infty$ ,  $x_1 = x_2 = 0$ , and from that point along the dashed line  $x_1 \rightarrow -\infty, x_2 \rightarrow +\infty$ , thus revealing the two-humped transverse structure of the surface wave. Note that the forward (backward) wave in linear case remains forward (backward) in nonlinear case, i.e. the type of the mode is determined by the linear parameters of the system and can be found using the diagram in Fig. 1.

### B. Nonlinear LH/linear RH interface

Next, we consider the surface waves propagating along an interface between linear RH and nonlinear LH media (see the inset in Fig. 4) having the negative nonlinear coefficient  $\alpha_2$  and, thus, displaying the self-focusing properties. The transverse structure of the stationary surface

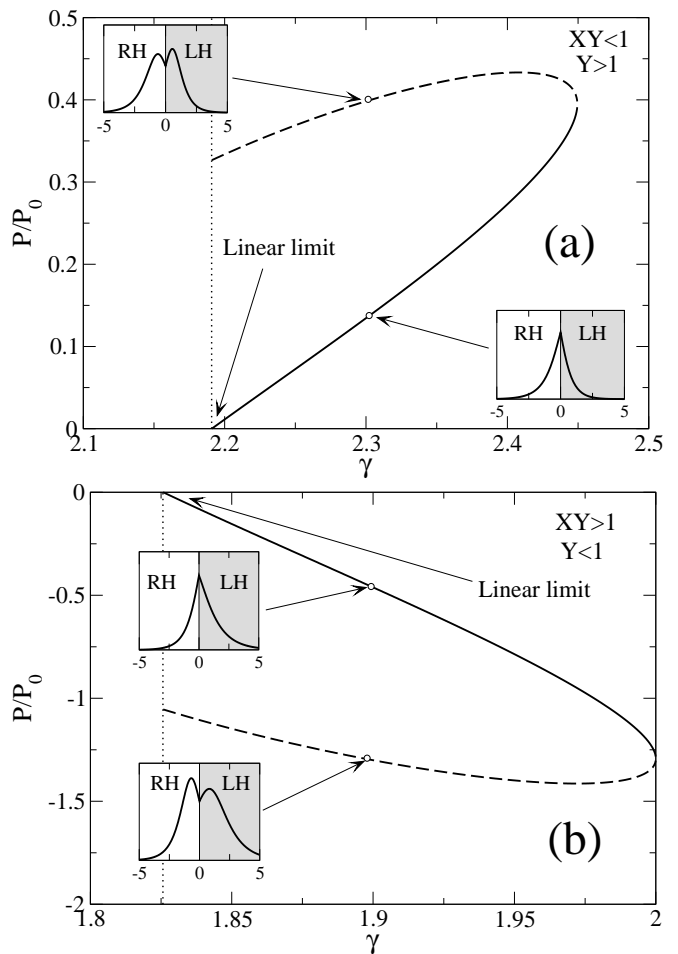


FIG. 3: Normalized energy flux vs. normalized wavenumber  $\gamma = hc/\omega$  for the nonlinear surface waves in two cases: (a)  $XY < 1, Y > 1$ , and (b)  $XY > 1, Y < 1$ . Solid curve corresponds to a one-humped structure, dashed – double-humped structure. The insets show the structure of the surface waves at the points indicated by arrows. Dotted lines denote the linear surface wave wavenumber.

wave has the form:

$$\Psi(x) = \begin{cases} E_0 \exp(\eta_1 x), & x < 0, \\ (2/\alpha_2 \mu_2)^{1/2} \eta_2 \operatorname{sech}[\eta_2(x - x_0)], & x > 0, \end{cases} \quad (24)$$

where  $E_0$  and  $x_0$  are two parameters which should be determined from the continuity conditions at the interface for the tangential components of the electric and magnetic fields,

$$\begin{aligned} \tanh(\eta_2 x_0) &= \mu_2 \eta_1 / (\mu_1 \eta_2), \\ E_0 &= (2/\alpha_2 \mu_2)^{1/2} \eta_2 \operatorname{sech}(\eta_2 x_0). \end{aligned} \quad (25)$$

Analyzing the relations (25), we find that a surface wave always has the maximum of the field intensity at the interface. This is in a sharp contrast to the nonlinear surface waves excited at the interface separating two RH media, when the electric field has maximum shifted into a self-focusing nonlinear medium [14].

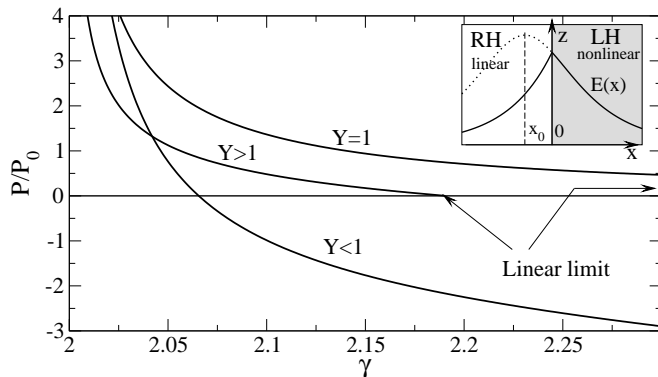


FIG. 4: Normalized energy flux *vs* normalized wavenumber  $\gamma = hc/\omega$  for the nonlinear surface waves at the nonlinear LH/Linear RH interface. Surface waves can be both forward (positive energy flux) and backward (negative energy flux). The inset shows the geometry of the problem.

The corresponding nonlinear dispersion relation of the surface waves is found in the form

$$\frac{\eta_1}{\mu_1} + \frac{\eta_2}{\mu_2} \left(1 - \frac{A_1^2}{\eta_2^2}\right)^{1/2} = 0, \quad (26)$$

where  $A_1 = E_0(\alpha_1\mu_1/2)^{1/2}$  is the normalized electric field amplitude at the interface. Equation (26) reduces to the linear dispersion relation (8) in the small-amplitude limit, i.e. when  $A_1 \rightarrow 0$ .

The energy flux  $P$  associated with the nonlinear surface wave can be calculated in the form

$$P = P_0\gamma\eta_2 \left(1 + \frac{\mu_2\eta_1}{\mu_1\eta_2}\right) \left[\frac{2}{\mu_2} + \frac{\eta_2}{\eta_1\mu_1} \left(1 - \frac{\mu_2\eta_1}{\mu_1\eta_2}\right)\right],$$

where  $P_0$  is defined above.

As an example, we consider the case  $XY < 1$  for which, as we have shown above, only forward surface waves can exist at the interface between two linear media. However, nonlinear surface waves can be both forward and backward, as demonstrated in Fig. 4. For  $Y < 1$ , there exists *no linear limit* for the existence of the surface waves, while in other two regions the results for linear surface waves are recovered in the limit  $P \rightarrow 0$ . The point on the curve corresponding to  $P = 0$  in the case  $Y < 1$  describes the wave of finite amplitude in which the energy flows on either side of the interface are balanced. Such a wave does not exist in the linear limit.

### C. Linear LH/nonlinear RH interface

Finally, we consider the case when the LH material is linear, while the RH medium is nonlinear. In such a geometry, the dispersion relation for the TE-polarized waves has the form

$$\frac{\eta_2}{\mu_2} + \frac{\eta_1}{\mu_1} \left(1 - \frac{A_2^2}{\eta_1^2}\right)^{1/2} = 0, \quad (27)$$

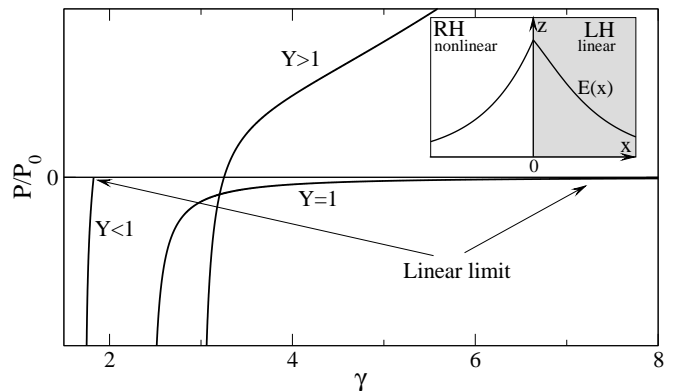


FIG. 5: Normalized energy flux *vs* normalized wavenumber  $\gamma = hc/\omega$  for the nonlinear surface waves at the linear LH/nonlinear RH interface. Surface waves can be both forward (positive energy flux) and backward (negative energy flux). The inset shows the geometry of the problem.

where  $A_2 = E_0\sqrt{\alpha_2\mu_2/2}$  is the normalized amplitude of the electric field at the interface.

The dependence of the normalized energy flux on the wave number of the surface wave is shown in Fig. 5 for  $XY > 1$ . In contrast to the linear waves, the nonlinear surface waves can be both forward and backward (see Fig. 1). In analogy with the case  $Y < 1$  for the nonlinear LH/linear RH interface, it can be shown that there exists no small-amplitude limit for the nonlinear surface waves for  $Y > 1$ . For  $XY < 1$  only forward travelling waves exist at  $Y > 1$ , revealing the property of the corresponding linear waves.

## IV. FREQUENCY DISPERSION OF NONLINEAR SURFACE WAVES

The group velocity of surface waves propagating along the interface is determined in a standard way through the slope of the dispersion curve,  $v_g = \partial\omega/\partial h|_{\omega_0}$ , where  $\omega_0$  is the carrier frequency of the surface wavepacket. As is shown below, the energy flow in the surface wave is proportional to the group velocity. The analysis of a change of the slope of the dispersion curve as a function of the dielectric permittivity in the vicinity of the critical value  $\epsilon_c$  (see Fig. 2) suggests that we can change the type of the surface wave from the forward to backward wave which can be controlled by the change of the amplitude of the electric field when the RH material becomes nonlinear. To demonstrate this property, we study the properties of nonlinear surface waves near the critical point and select  $\epsilon_1 = 3.4$ , in order to stay just below the critical value  $\epsilon_c$  corresponding to the linear case.

It should be mentioned here that although the negative permeability of the LH composite material is necessary for the existence of TE surface waves in the present model, it has been shown [15] that the TE surface waves do exist at the interface between a RH nonlinear plasma

and a RH nonlinear dielectric medium with a constant zero-field permittivity, provided that the nonlinear parameter in the plasma exceeds that in the dielectric medium. In that case, since  $\mu = 1$  in both media, it has also been shown [15] that the relation between the wave intensity at the boundary and the frequency are independent of the wave number. In the present case, where the LH composite material has a permeability not equal to unity, this result is no longer valid. In our problem, Eq. (27) provides a dependence between the three variables  $h$ ,  $A_2$  and  $\omega$ , so that the wave intensity at the boundary depends on both  $h$  and  $\omega$ .

As was shown for the case of linear surface waves, a change of the slope of the dispersion curve takes place at the critical value of dielectric permittivity of the RH medium (13). In the nonlinear case, the dielectric permittivity of the RH medium depends on the field intensity and, in particular, it exceeds the critical value when the wave amplitude  $A_2$  becomes larger than the threshold value  $A_{2c}$  given by the equation

$$A_{2c}^2 = \left(\frac{\omega_p}{\omega_0}\right)^2 \left(1 - \frac{F}{2}\right) - (1 + \epsilon_1). \quad (28)$$

For the media parameters used above, the equation (28) gives the results:  $A_{2c} = 0.3162$ . Figure 6 shows the dispersion curves for three different wave amplitudes. As was discussed above, the slope of the curves is positive for the wave amplitudes below the critical value (28), and it is negative, otherwise. One can also notice from Fig. 6 that the existence region for the surface waves depends on the wave amplitude  $A_2$ . In Fig. 7 we present this existence region on the plane of the wave amplitude and normalized frequency. The existence region of the backward surface waves below the critical value collapses at  $A_{2c}$ , and it expands in the region of the forward surface waves above the threshold. Note, that the forward and backward waves exist at different frequencies only.

The existence regions of the surface wave can be explained from the viewpoint of the physics of wave localization. The wave localization is determined by the normalized transverse wavenumbers  $\eta_{1,2}$ . As was mentioned above, these wavenumbers define the inverse decay length of the surface wave in the corresponding medium. The condition  $\max\{\eta_1, \eta_2\} = 0$  corresponds to the delocalized waves, and it determines the boundary of the wave existence. Figure 8 shows the dependence of the normalized wave number on the wave amplitude for different frequencies. These curves represent the horizontal cross-sections of the region of the wave existence shown in Fig. 7. The dashed line in Fig. 8 shows the boundary of localization of the wave in the LH material. Comparing Fig. 8 and Fig. 7, we come to the conclusion that in Fig. 7 the upper boundary for the existence of the forward waves (below  $A_{2c}$ ) and the lower boundary for the backward wave existence (above  $A_{2c}$ ) are determined by the wave localization in the LH material.

The power flow in the linear LH composite medium is

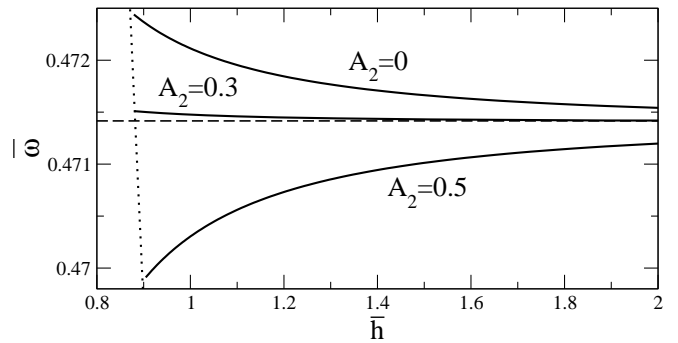


FIG. 6: Normalized frequency vs. normalized wave number for different values of the amplitude  $A_2$ . Dashed line corresponds to the line  $\omega_1$  in Fig. 2; dotted line is  $\eta_2 = 0$ .

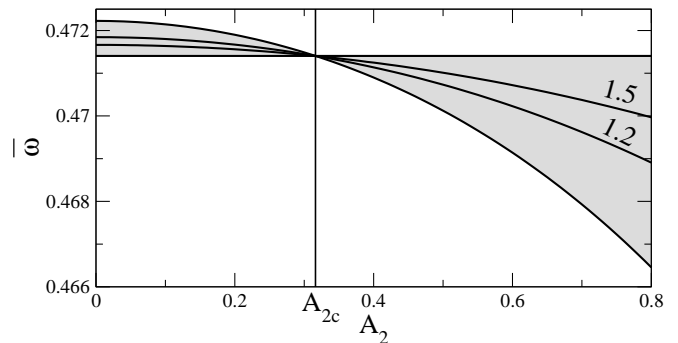


FIG. 7: Existence region of nonlinear surface waves (shaded). The curves show the amplitude  $A_2$  vs. normalized frequency, for different values of the normalized wave number (marked at the curves). All curves intersect at the critical point  $A_2 = A_{2c}$ .

given by the result

$$P_2 = \frac{c^2 \gamma}{16\pi\omega\mu_2\eta_2} E_0^2, \quad (29)$$

and, using the boundary value technique [14], the power flow in the nonlinear half-space (RH medium) can be obtained in the following form

$$P_1 = \frac{c^2 \gamma}{4\pi\omega\mu_1^2\alpha_1} \left( \eta_1 - \sqrt{\eta_1^2 - E_0^2 \frac{\alpha_1\mu_1}{2}} \right). \quad (30)$$

We notice here that, although the nonlinear coefficient  $\alpha_1$  appears as a factor in the denominator of Eq. (30), the reduction to the linear case (when  $\alpha_1 \rightarrow 0$ ) can be performed in a straightforward way by expanding Eq. (30) as for small  $\alpha_1$  as follows

$$P_1 \rightarrow \frac{c^2 \gamma}{4\pi\omega\mu_1^2\alpha_1} \left[ \eta_1 - \left( \eta_1 - \frac{E_0^2\alpha_1}{4c^2\eta_1} + O(\alpha_1^2) \right) \right] \quad (31)$$

i.e.

$$P_1 \rightarrow \frac{c^2 \gamma}{16\pi\omega\mu_1\eta_1} E_0^2, \quad (32)$$

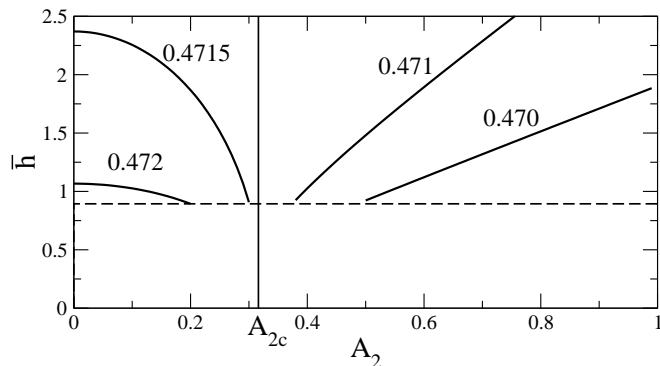


FIG. 8: Normalized wave number vs. normalized field amplitude  $A_2$ , for different frequencies. Dashed line is  $\eta_2 = 0$ . The curves on the left of  $A_{2c}$  meet the wave number axis at the values corresponding to the linear case. There exist no linear solutions to the right of the critical vertical line  $A_2 = A_{2c}$

which coincides with Eq. (29).

The absolute value of the ratio of the power flow in the RH nonlinear medium to the power flow in the LH composite medium is depicted in Fig. 9. Above the critical value  $A_c$ , there always exists a value of the wave number at which the power flow is positive. In this region, there exist a forward travelling surface wave. Note that no matter what the value of the field intensity at the boundary is, there exists always some value of the wave number where the flow is negative and there exists a backward travelling surface wave. This can be seen by reference to Eq. (29). The presence of  $\eta_2$  in the denominator of Eq. (29) means that as  $h$  approaches a value that makes  $\eta_2 = 0$  (i.e. a dispersion curve in Fig. 6 approaches the dashed line) the negative power flow in the LH material dominates the total power flow. Conversely, as  $\eta_2$  increases from zero, the negative power flow in the LH medium decreases so that, provided the intensity of the electric field at the boundary is high enough, the positive power flow in the nonlinear dielectric dominates.

## V. PULSE PROPAGATION AND SURFACE-WAVE SOLITONS

### A. Envelope equation

Propagation of pulses along the interface between RH and LH media is of a particular interest, since we have shown above that the energy fluxes are *directed opposite* at either side of the interface. Therefore, we can expect that the energy flow in a pulse has a nontrivial form and, in particular, it can be associated with a vortex-like structure of the energy flow.

We analyze the structure of surface waves of both temporal and spatial finite extensions that can exist in such a geometry. To obtain the equation describing the pulse propagation along the interface, we look for the structure of a broad electromagnetic pulse with the carrier

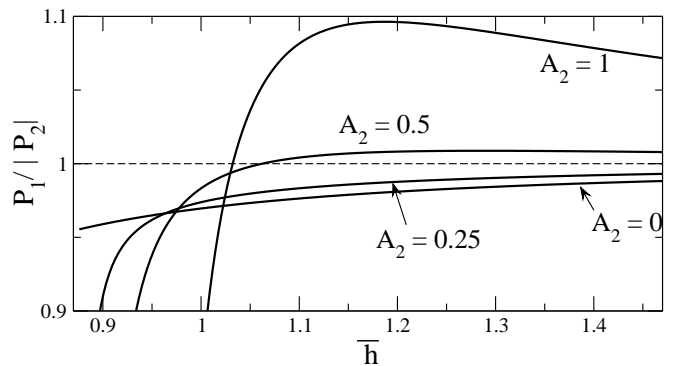


FIG. 9: The absolute value of the ratio of the power flow in the nonlinear dielectric to that in the LH material. Above the critical value  $A_c$ , the power flow in the nonlinear half-space dominates giving a forward travelling wave. As  $\kappa_2$  approaches zero towards the left-hand side of the curves, the power in the left-handed medium dominates.

frequency  $\omega_0$  described by an asymptotic multi-scale expansion with the main terms of the general form

$$\Psi = e^{ih_0z - i\omega_0t} \left[ \Psi_0(x)A(\xi, t) - i\Psi_1(x)\frac{\partial A(\xi, t)}{\partial \xi} + \Psi_2(x, \xi, t) + \dots \right], \quad (33)$$

where the field  $\Psi$  stands for the components  $(E_y, H_x, H_z)$  of a TE-polarized wave, the first term  $\Psi_0 = (E_{y0}, H_{x0}, H_{z0})$  describes the structure of the mode at the carrier frequency  $\omega_0$ ,  $\Psi_1$  is the first-order term of the asymptotic series which can be found as  $\Psi_1 = \partial\Psi_0/\partial h$ , and  $\Psi_2$  is the second-order term. Here  $A$  is the pulse envelope,  $h_0$  is the wave number corresponding to the carrier frequency  $\omega_0$ ,  $\xi = z - v_g t$  is the pulse coordinate in the reference frame moving with the group velocity  $v_g = \partial\omega/\partial h$ . Substituting Eq. (33) into Eq. (5) and using the Fredholm alternative theorem, one can obtain the well-known equation for the evolution of the field envelope

$$i\frac{\partial A}{\partial t} + \frac{\delta}{2}\frac{\partial^2 A}{\partial \xi^2} = 0; \quad (34)$$

where the coefficient  $\delta = \partial^2\omega/\partial h^2$  stands for the group-velocity dispersion which can be calculated from the dispersion relations. As usual, the group-velocity dispersion determines the pulse broadening.

### B. Vortex-like energy flow

In order to study the energy flow associated with the pulse propagation along the interface, we present the electric and magnetic fields of the pulse as follows

$$\begin{aligned} \mathbf{E} &= \frac{1}{2} [\mathbf{E}(\mathbf{t}) \exp(-i\omega_0 t) + c.c], \\ \mathbf{H} &= \frac{1}{2} [\mathbf{H}(\mathbf{t}) \exp(-i\omega_0 t) + c.c], \end{aligned} \quad (35)$$

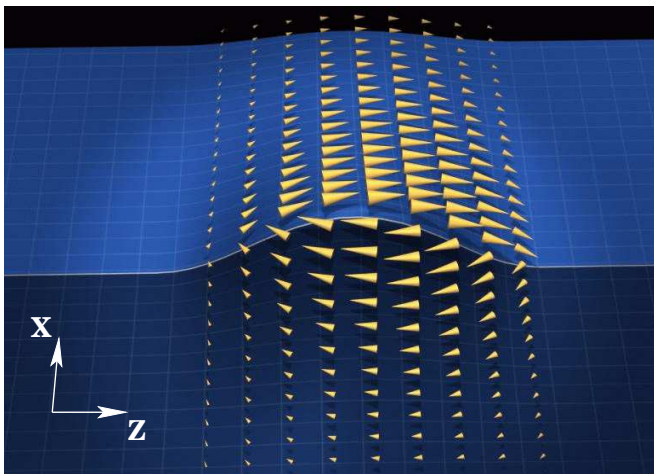


FIG. 10: A vortex-like distribution of the Poynting vector in a surface wave packet propagating along the LH/RH interface.

where the complex amplitudes  $(\mathbf{E}(\mathbf{t}), \mathbf{H}(\mathbf{t}))$  are slowly varying functions on the scale of the period of the carrier frequency  $T = 2\pi/\omega_0$ , and *c.c.* stands for the complex conjugate. Thus, the surface-wave pulse is assumed to have a narrow spectrum in the vicinity of the carrier frequency  $\omega_0$ . Then, the Poynting vector can be written in the form of the expansion

$$\mathbf{S} = \frac{c}{16\pi} [\mathbf{E}(\mathbf{t}) \times \mathbf{H}(\mathbf{t}) \exp(-2i\omega_0 t) + \mathbf{E}(\mathbf{t}) \times \mathbf{H}^*(\mathbf{t}) + c.c.], \quad (36)$$

Integrating this expression over the period  $T$ , we neglect changes of the envelope functions on that scale and finally obtain Eq. (14), where both the electric and magnetic complex amplitudes are the slowly varying functions of time. Using the asymptotic expansions (33) for the field components, we obtain the energy flow structure described by their components

$$S_z = \frac{c^2 h_0}{8\pi\omega_0\mu} E_0^2 |A|^2, \quad (37)$$

$$S_x = \frac{c^2}{8\pi\omega_0\mu} \left[ \frac{\partial E_0}{\partial h} \frac{\partial E_0}{\partial x} - E_0 \left( \frac{\partial^2 E_0}{\partial h \partial x} - \frac{v_{gr}}{\omega_0} \frac{\partial E_0}{\partial x} \right) \right] \text{Re} \left( A \frac{\partial A^*}{\partial \xi} \right) \quad (38)$$

The structure of the Poynting vector in the surface-wave pulse is shown in Fig. (10), where it is clearly seen that the energy rotates in the localized region creating a vortex-type energy distribution in the wave. The difference between the Poynting vector  $|S_z|$  integrated over the RH medium and that calculated for the LH medium determines the resulting group velocity of the surface wave packet.

We notice that the distinctive vortex-like structure of the surface waves at the interface separating RH and LH media follows as a result of the opposite signs of the dielectric permittivity for the TM-polarized waves and the

magnetic permittivity for the TE-polarized waves. These conditions coincide with the conditions for the existence of the corresponding surface waves and, therefore, surface polaritons associated with the LH media should always have such a distinctive vortex-like structure.

### C. Surface-wave solitons

The existence of the surface polariton solitons has been predicted in a number of structures supporting nonlinear guided waves (see, e.g., Ref. [16] and references therein). The corresponding nonlinear equation for describing the evolution of the field amplitude  $A$  at the interface is known to have the form of the nonlinear Shrödinger (NLS) equation,

$$i \frac{\partial A}{\partial t} + \frac{\delta}{2} \frac{\partial^2 A}{\partial \xi^2} - \omega_2(h) |A|^2 A = 0; \quad (39)$$

where  $\omega_2(h) = (\partial\omega_{NL}/\partial A^2)|_{A=0}$  is the effective nonlinear coefficient calculated with the help of the nonlinear dispersion relation. As is well-known, the NLS equation has a solution in the form of a bright soliton localized at the interface, provided the GVD has the opposite sign to the sign of the nonlinear coefficient  $\omega_2$ . In our problem, we calculate the effective nonlinear coefficient for the case of an interface between the nonlinear LH medium and the linear RH medium, using Eq. (25):

$$\omega_2(h) = -\frac{\alpha\mu_1\kappa_1\kappa_2\omega^2}{4hc^2(\epsilon_2\mu_2 - \epsilon_1\mu_1)} \frac{d\omega}{dh}. \quad (40)$$

The signs of the group velocity  $d\omega/dh$  and of the parameter  $\delta$  can be determined from the Fig. 2. As a result, for any reasonable values of dielectric permittivity and magnetic permeability of the RH medium, there exists a range of frequencies for which  $\omega_2 \cdot \delta < 0$ , indicating the possibility of exciting surface polariton solitons.

## VI. CONCLUSIONS

We have presented a systematic study of both linear and nonlinear surface waves supported by an interface between a left-handed metamaterial and a conventional dielectric medium. For the linear regime, we have extended some earlier theoretical results and analyzed different types of surface waves and their existence regions. In particular, we have demonstrated that the structure of the energy flow in a spatially localized wave-packet of the surface waves propagating along the interface has a vortex-like structure. For the case of nonlinear surface waves, we have demonstrated that when only one of the media is nonlinear the maximum amplitude of the spatially localized wave does not shift out the interface. This result is in a sharp contrast to the case of an interface between linear and nonlinear right-handed materials where the maximum of a surface wave is always shifted into a

self-focusing nonlinear medium. We have demonstrated that the group velocity of nonlinear surface waves can be controlled by changing the intensity of the electromagnetic field and, in particular, the surface wave can be switched from the forward propagating one to the back-

ward propagating one by varying the field intensity only. In addition, we have obtained the conditions for the existence of the surface-polariton solitons at the metamaterial interface.

---

\* URL: <http://wwwrphysse.anu.edu.au/nonlinear/>

- [1] V. G. Veselago, Usp. Phys. Nauk **92**, 517 (1967).
- [2] D. R. Smith, W. Padilla, D. C. Vier, S. C. Nemat-Nasser, and S. Shultz, Phys. Rev. Lett. **84**, 4184 (2000).
- [3] L. Venema, Nature **420**, 119 (2002).
- [4] J. B. Pendry, Phys. Rev. Lett. **85**, 3966 (2000).
- [5] C. Luo, S. G. Johnson, J. D. Joannopoulos, and J. B. Pendry, Phys. Rev. B **65**, 201104 (2002).
- [6] R. Ruppin, Phys. Lett. A **277**, 61 (2000).
- [7] J. B. Pendry, A. J. Holden, W. J. Stewart, and I. Youngs, Phys. Rev. Lett. **76**, 4773 (1996).
- [8] Y. I. Bespyatyh, A. S. Bugaev, and I. E. Dickshtein, Fizika Tverdogo Tela **43**, 2043 (2001).
- [9] F. D. M. Haldane, arXiv:cond-mat/0206420 (2002).
- [10] A. D. Boardman, ed., *Electromagnetic surface modes* (New York : Wiley, 1982).
- [11] R. Ruppin, J. Phys. Condens. Matter **13**, 1811 (2001).
- [12] A. G. Litvak and V. A. Mironov, Izv. Vuzov: Radiophysica **11**, 1911 (1968).
- [13] A. A. Zharov, I. V. Shadrivov, and Yu. S. Kivshar, arXiv:cond-mat/0303443 (2003).
- [14] A. D. Boardman and P. Egan, IEEE J. Quant. Electron. **10**, 1701 (1985).
- [15] A. A. Maradudin, Z-Phys – Condens. Matter **41**, 341 (1981).
- [16] A. D. Boardman, G. S. Cooper, A. A. Maradudin, and T. P. Shen, Phys. Rev. B **34**, 8273 (1986).